of 40° for example of the following conditions: 1) $M_\infty = 3.1795$, 2) $T_s/T_0 = 0.05$, 3) $\theta_c = 15°$, and 4) $\alpha = 10°$. The external flow parameters used are based upon first-order theory. The results are shown in Table 1, which also includes the results of calculation on coefficient of friction, coefficient of friction in x direction, shear parameter f_w'', angle between total coefficient of friction and coefficient of friction in x direction, and Stanton number St. In the circumferential direction off the stagnation line (i.e., as ϕ increases) 1) the coefficient of friction in the x direction and f_w'' decrease, 2) the coefficient of friction in the x direction increases since it is directly proportional to b, 3) the total coefficient of friction decreases, and 4) the angle between the total coefficient of friction and that in the x direction increases. Comparisons are made of the distribution of heat transfer coefficient in the circumferential direction and that obtained by experiments. The present theoretical results are found to agree fairly well with the available experimental data for similar flow conditions. Two such comparisons are shown in Figs. 2 and 3. The experimental results in Fig. 2 are for much higher Mach number, and other flow parameters are slightly different.[7] The experimental results for Fig. 3 are for a yawed cylinder.

Discussion

The results on coefficients of friction and friction parameters are of special interest, since neither experimental data nor theoretical results on those are available. Any experimental data on coefficients of friction which may become available for a cone at angles of attack for comparison with the theoretical results obtained will be helpful in establishing the accuracy of the present method to investigate the complete boundary layer characteristics around a cone at angles of attack. The variation of K also should be considered in extending the calculation to the case of larger circumferential angles; however, it should be pointed out that the accuracy of the integral method suffers on the leeward side of the yawed cone which has an unfavorable pressure gradient. Furthermore, at large angles of attack, the boundary layer on the leeward side no longer can be considered as thin.

References

[1] Moore, F. K., "Laminar boundary-layer on a cone in supersonic flow at large angle of attack, "NACA TN 2844 (November 1952).

[2] Brunk, W. E., "Approximate method for calculation of laminar boundary-layer with heat-transfer on a cone at large angle of attack in supersonic flow," NACA TN 4380 (September 1958).

[3] Reshotko, E. and Beckwith, I. E., "Compressible laminar boundary-layer over a yawed infinite cylinder with heat-transfer and arbitrary Prandtl number," NACA TN 3986 (June 1957).

[4] Reshotko, E., "Laminar boundary-layer with heat-transfer on a cone at angle of attack in a supersonic stream," NACA TN 4152 (December 1957).

[5] Burbank, P. B. and Hodge, B. L., "Distribution of heat-transfer on a 10° cone at angles of attack from 0° to 15° for Mach numbers of 2.49 to 4.65 and a solution to the heat-transfer equation that permits complete machine calculations," NASA Memo. 6-4-59L (June 1959).

[6] Conti, R. J., "Laminar heat-transfer and pressure measurements at a Mach number of 6 on sharp and blunt 15° half-angle cones at angles of attack up to 90°, NASA TN D-962 (October 1961).

[7] Wittliff, C. E. and Wilson, M. R., "Heat-transfer to slender cones in hypersonic air flow including yaw and nose-bluntness effects," Cornell Aeronaut. Lab. Paper 61-213-1907 (June 1961).

[8] Goodwin, G., Creager, M. O., and Winkler, E. L., "Investigation of local heat-transfer and pressure drag characteristics of a yawed circular cylinder at supersonic speeds," NACA RM A55 H31 (January 1956).

[9] Sands, N. and Jack, J. R., "Preliminary heat-transfer studies on two bodies of revolution at angle of attack at a Mach number of 3.12," NACA TN 4378 (September 1958).

[10] Kopal, Z., "Tables of supersonic flow around cones of large yaw," TR 5, Dept. Elect. Eng., Mass. Inst. Tech. (1949).

[11] Kopal, Z., "Tables of supersonic flow around yawing cones," TR 3, Dept. Elect. Eng., Mass. Inst. Tech. (1947).

[12] Yen, S. M., "Investigation of laminar heat-transfer and skin friction on a slender cone at angles of attack," McDonnell Aircraft Corp. Rept. 7086 (September 1959).

MARCH 1963 AIAA JOURNAL VOL. 1, NO. 3

Some Exact Solutions for Cavitating Curvilinear Bodies

Fredric F. Ehrich*

General Electric Company, West Lynn, Mass.

A special case of cavitating flow solutions is postulated and transformed to a semi-infinite plane. The complete, exact solution then is synthesized by superposition of singularities. The solution is relevant to a general, two-parameter family of curvilinear bodies. The parameters are the flow angles at the two points of flow separation. The body reduces, in the special case, to the Rayleigh solution for a flat plate. The equations of the cavity boundaries are given in explicit form. The body form and the stagnation streamline are given as the locus of the roots of a cubic equation. Local static pressures and, hence, lift and drag, also may be calculated. The generated solutions constitute a technique involving simple computation for exact solutions of a special family of cavitating curvilinear bodies at finite angles of attack.

Nomenclature

a, b, A, B, C, E	=	solution constants
A, B, C, D, E, F	=	labels of locations in various planes
C_D	=	drag coefficient
C_L	=	lift coefficient
c	=	chord length
$R = (\xi^2 + \eta^2)^{1/2}$	=	radial vector length in the ζ plane
r_1, r_2	=	location of the singularities in the ζ plane
s_1, s_2, s_3	=	location of stagnation points in the ζ plane
$w = \phi + i\psi$	=	complex potential (potential function, stream function)
$z = x + iy$	=	complex physical coordinate (abscissa, ordinate)
$\zeta = \xi + i\eta$	=	complex half-plane coordinate (abscissa, ordinate)

Received by IAS August 10, 1962; revision received December 26, 1962.

* Engine Design Engineer, Small Aircraft Engine Department.

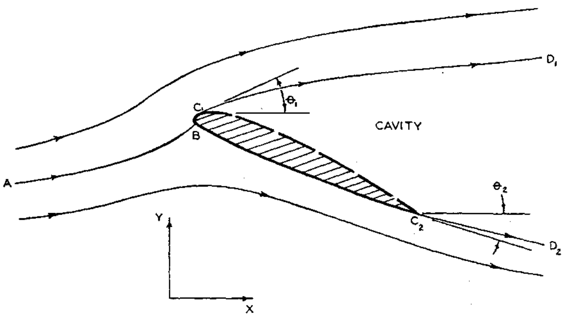

Fig. 1 Physical plane, cavitating curvilinear body ($z = x + iy$)

θ = streamline inclination
$\nu = u - iv$ = complex conjugate hodograph plane (horizontal velocity component, vertical velocity component)

Introduction

EXCEPT for the well-known Rayleigh[1] solution for a flat plate at arbitrary angle of attack and the case of a symmetric cavity in an infinite stream given by Birkhoff and Zarantonello,[2] the general fluid dynamic solution to the cavitating body of arbitrary shape generally is not available because of the nonlinear nature of the problem. Certain exact solutions are given by Greenhill.[3] Engineering interest in supercavitating propellers and hydrofoil elements has fostered considerable investigation in recent years in this area. Recent results are typified by Tulin's and Burkart's[4] linearization of the problem and Wu's[5] generalization of the Levi-Civita method.

Taking example from the Joukowski family of airfoils, it would seem desirable to *synthesize* a specialized family of simple exact solutions to the cavitating curvilinear body problem by superposition of singularities. Although artificial synthesis does not necessarily lead to systematically predictable shapes, it does provide a reference for more general approximate theories or experiments, and its detailed result may sometimes supplement general insight.

Consider the cavitating body of Fig. 1. Make the conventional assumptions of inviscid, irrotational, two-dimensional flow, with constant static pressure streamlines delineating the cavity at a vapor cavitation number of zero.

Mapping

The conjugate of the complex hodograph of the flow field (Fig. 2) is related analytically to the complex potential and the complex physical coordinates by the relationship

$$\nu = -dw/dz = u - iv \tag{1}$$

Fill in a matching flow field in the hodograph plane (stippled

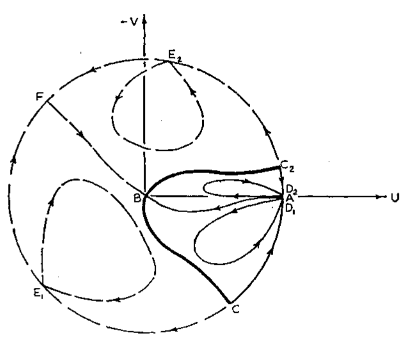

Fig. 2 Complex conjugate hodograph plane ($\nu = u - iv$)

in Fig. 2) to complete a full circle. The flow within this circle may be transformed directly into a half plane (Fig. 3) by the transformation

$$\zeta = i(1 - \nu)/(1 + \nu) = \xi + i\eta \tag{2a}$$

or, in inverted form,

$$\nu = -(\zeta - 1)/(\zeta + i) \tag{2b}$$

Relative position of the singularities and stagnation points is given in Fig. 4, where infinity may be taken at any point on the cyclic sequence. Points on the free streamlines transform as

$$\zeta = -\tan(\theta/2) \tag{3}$$

where $\nu = e^{-i\theta}$, and the central stagnation point gives

$$\zeta = i \tag{4}$$

where $\nu = 0$.

Synthesis

The flow in this half plane may be synthesized by the transformation that relates it to the complex potential function:

$$\frac{dw}{d\zeta} = \frac{(\zeta^2 + 1)(\zeta - s_1)(\zeta - s_2)(\zeta - s_3)}{\zeta^3(\zeta - r_1)^2(\zeta - r_2)^2} \tag{5}$$

which gives the field the following essential properties:

1) The flow has stagnation points in the ζ plane at ζ equal to s_1, s_2, s_3, and i.

2) The real axis in the ζ plane is a boundary, since the velocity along it has no vertical (i.e., imaginary) component.

3) On integrating the expression, it gives a second-order singularity (quadrupole) in the ζ plane at the origin. This has the distinctive four lobes necessary to synthesize the required picture (i.e., two lobes above and two lobes below the horizontal axis).

4) Integration also gives first-order singularities (dipoles) in the ζ plane at r_1 and r_2. These have the distinctive two lobes necessary to synthesize the flow in the vicinity of these points (i.e., one lobe above and one symmetric lobe below the axis at each of the singularities).

Integrating this expression gives the explicit form

$$w = \frac{A_3\zeta^3 + A_2\zeta^2 + A_1\zeta + A_0}{\zeta^2(\zeta - r_1)(\zeta - r_2)} \tag{6}$$

where sources and sinks (logarithmic forms) purposely have been excluded as being inappropriate to the required solution form. Differentiate this expression and match coefficients of the fifth-order numerator polynomial with that of Eq. (5). This gives six equations in A_0, A_1, A_2, A_3, r_1, r_2, s_1, s_2, and s_3.

On close examination of this solution, it appears that, although it meets criteria 1–4, it gives some flows that are more complex than the picture in Fig. 3 and are not appropriate to the required synthesis. A further restriction must be placed on the transformation—that the stagnation points must be on the same streamline:

$$\psi(i) = \psi(s_1) = \psi(s_2) = 0 \tag{7}$$

This leads to another restrictive equation in A_0, A_1, A_2, A_3, r_1, and r_2.

The resultant total of seven equations permits a solution to be found for A_0, A_1, A_2, A_3, r_1, r_2, and s_3 in terms of s_1 and s_2. That is, for an arbitrary selection of the leading and trailing edge flow separation angles, the location of the last stagnation point and the locations of the doublets in the ζ

plane may be computed, and the integration of the $w(\zeta)$ transformation may be completed.

The stagnation point locations in the ζ plane are related to the selected leading and trailing edge flow separation angles:

$$s_1 = -\tan(\theta_1/2) \tag{8a}$$

$$s_2 = -\tan(\theta_2/2) \tag{8b}$$

The location of the last stagnation point in the ζ plane is found to be

$$s_3 = -(s_1 s_2 + 3)/(s_1 + s_2) \tag{8c}$$

These stagnation points can be used to determine the coefficients

$$a_1 = s_1 + s_2 + s_3 \tag{9a}$$

$$a_3 = s_1 s_2 s_3 \tag{9b}$$

which permit solution for the parameters

$$b_1 = r_1 + r_2 = -4/(a_1 + a_3) \tag{10a}$$

$$b_2 = r_1 r_2 = 2a_3/(a_1 + a_3) \tag{10b}$$

Then

$$r_1 = (b_1/2) - [(b_1/2)^2 - b_2]^{1/2} \tag{11a}$$

$$r_2 = (b_1/2) + [(b_1/2)^2 - b_2]^{1/2} \tag{11b}$$

The doublet and stagnation point locations must be taken in terms of cyclic sequence implied by Fig. 4, with complex solutions to Eq. (11) disallowed.

Finally, the complex potential function is found to be

$$w = \frac{(\zeta^2 + 1)^2}{(-b_1)\zeta^2(\zeta - r_1)(\zeta - r_2)} \tag{12}$$

when adjusted by an additive constant.

Physical Plane

One may complete the analysis by relating the flows in the planes already analyzed to the flow in the physical plane. From Eq. (1) one finds

$$dz/d\zeta = -(dw/d\zeta)/\nu \tag{13}$$

Introducing Eq. (2b) and Eq. (5), one gets

$$dz = \frac{(\zeta + i)^2(\zeta - s_1)(\zeta - s_2)(\zeta - s_3)}{\zeta^3(\zeta - r_1)^2(\zeta - r_2)^2}\, d\zeta \tag{14}$$

which may be integrated to give

$$z = \frac{B_3\zeta^3 + B_2\zeta^2 + B_1\zeta + B_0}{\zeta^2(\zeta - r_1)(\zeta - r_2)} + C_0\ln\zeta + C_1\ln(\zeta - r_1) + C_2\ln(\zeta - r_2) \tag{15}$$

Differentiating Eq. (15) and matching coefficients with Eq. (14) permits direct computation of the coefficients to express the integration in terms of the problem parameters as the solution to the set of complex simultaneous equations:

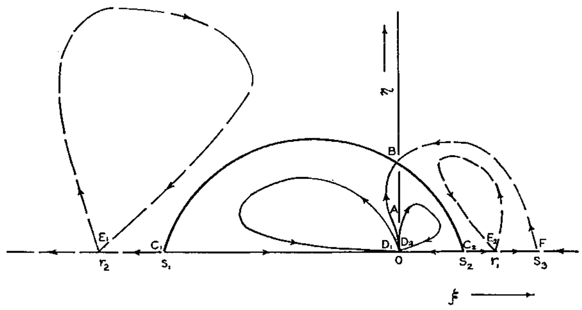

Fig. 3 Mapping half plane ($\zeta = \xi + i\eta$)

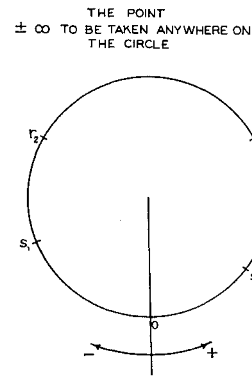

Fig. 4 Cyclic order of the location of the singularities on the ξ axis

Numerical Solution

For selected values of r_1 and r_2, the transformations $w(\zeta)$ in Eq. (6) and $z(\zeta)$ in Eq. (15) constitute a complete physical description of the flow field parametrically in ζ. The local velocity (and hence local static pressures by Bernoulli's equation) are given by $\nu(\zeta)$ in Eq. (2b).

The shape of the free streamlines is given by substitution of *real* values of ζ, taken in the algebraic sense of Fig. 4 and lying between 1) s_1 and 0 for the upper branch free streamline, and 2) s_2 and 0 for the lower branch free streamline.

The shapes 0 the solid body and the stagnation streamlines are characterized by the streamlines ($\psi = 0$), which can be determined as the locus of the roots of the equation

$$(2\xi)^3 + E_2(2\xi)^2 + E_1(2\xi) + E_0 = 0 \tag{17}$$

where

$$E_2 = -b_1 \tag{18a}$$

$$E_1 = (1 - R^2)[b_2(R^2 + 1) - 2R^2] \tag{18b}$$

$$E_0 = b_1 R^2(1 - R^2)^2 \tag{18c}$$

and

$$\eta^2 = R^2 - \xi^2 \tag{19}$$

The roots are taken in the sense of ζ lying on a line connecting 3) s_1 and i for the upper section of the body, 4) s_2 and i for the lower section of the body, and 5) 0 and i for the stagnation streamline.

Having derived the locus of body in the ζ plane, direct substitution in Eqs. (15) and (2b) gives the physical shape

$$\begin{bmatrix} 0 & 0 & 0 & 0 & 1 & 1 & 1 \\ 0 & 0 & 0 & -1 & 0 & r_1 & r_2 \\ 0 & 0 & -2 & -b_1 & b_2 & 0 & 0 \\ 0 & -3 & b_1 & 2b_2 & -b_1b_2 & 0 & 0 \\ -4 & 2b_1 & 0 & 0 & b_2^2 & 0 & 0 \\ 3b_1 & -b_2 & 0 & 0 & 0 & 0 & 0 \\ -2b_2 & 0 & 0 & 0 & 0 & 0 & 0 \end{bmatrix} \begin{Bmatrix} B_0 \\ B_1 \\ B_2 \\ B_3 \\ C_0 \\ C_1 \\ C_2 \end{Bmatrix} = \begin{Bmatrix} 0 \\ 1 \\ b_1 - a_1 \\ -b_2 - 4 \\ -a_3 + a_1 \\ 3 \\ a_3 \end{Bmatrix} + \begin{Bmatrix} 0 \\ 0 \\ 1 \\ -a_1 \\ -3 \\ -a_3 \\ 0 \end{Bmatrix} 2i \tag{16}$$

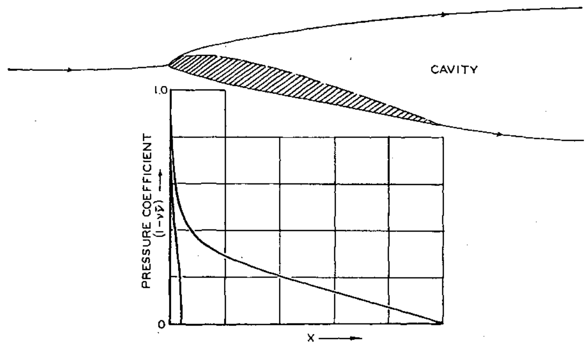

Fig. 5a Foil shape, stagnation streamline, free streamlines, and pressure distribution on the foil ($\theta_1 = 32.5°$, $\theta_2 = -10.3°$, $C_L = 0.172$, $C_D = 0.0680$)

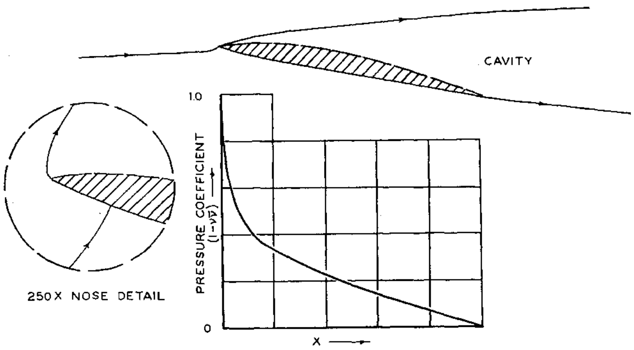

Fig. 5b Foil shape, stagnation streamline, free streamlines, and pressure distribution on the foil ($\theta_1 = 156.7°$, $\theta_2 = -9.8°$, $C_L = 0.225$, $C_D = 0.0484$)

and local velocities (and hence pressures). Lift and drag then may be computed by numerical integration:

$$C_L = \int_{C_2}^{C_1} (1 - \nu\bar{v}) d\left(\frac{x}{c}\right) \tag{20a}$$

$$C_D = \int_{C_1}^{C_2} (1 - \nu\bar{v}) d\left(\frac{y}{c}\right) \tag{20b}$$

Special Case: Flat Plate

When the flow angles of the separation are taken as

$$\theta_1 = -\theta \tag{21a}$$

$$\theta_2 = \pi - \theta \tag{21b}$$

giving stagnation points in the ζ plane

$$s_1 = \tan(\theta/2) \tag{22a}$$

$$s_2 = -\cot(\theta/2) \tag{22b}$$

then the dipoles are found to be coincident, forming a quadrupole at

$$r_1 = r_2 = s_3 = \tan\theta \tag{23}$$

The solution degenerates to the well-known Rayleigh[1] solution for the flat plate rotated θ clockwise from a horizontal (zero angle of attack) condition.

Special Case: Symmetric Body

When the separation angles are symmetric about a horizontal centerline,

$$\theta_1 = -\theta \tag{24a}$$

$$\theta_2 = \theta \tag{24b}$$

giving

$$s_1 = \tan(\theta/2) \tag{25a}$$

$$s_2 = -\tan(\theta/2) \tag{25b}$$

then the third stagnation point disappears, and the dipoles are found to be located symmetrically at

$$r_1 = -r_2 = r = [2s_1^2/(1 - s_1^2)]^{1/2} \tag{26}$$

The body form in the ζ plane is defined by the equation

$$\xi^2 = (1 - R^2)[r^2(R^2 + 1) + 2R^2]/4 \tag{27}$$

The body form then is found in the physical plane in terms of the general transformation $z(\zeta)$ of Eq. (15) with the coefficients evaluated as the limiting form of Eq. (16):

$$B_0 = -r^2 \tag{28a}$$

$$B_1 = 4r^2 i \tag{28b}$$

$$B_2 = r^4 \tag{28c}$$

$$B_3 = -2(1 - r^2)i \tag{28d}$$

$$C_0 = 4 \tag{28e}$$

$$C_1 = -2 - [(1 - r^2)i/r] \tag{28f}$$

$$C_2 = -2 + [(1 - r^2)i/r] \tag{28g}$$

Conclusions

Figure 5 depicts actual computed contours and streamlines for two typical foil shapes, Fig. 5a with detachment on the suction side ($\theta_1 = 32.5°$, $\theta_2 = -10.3°$), and Fig. 5b with detachment on the pressure side ($\theta_1 = 156.7°$, $\theta_2 = -9.8°$). The computed pressure distributions for these particular solutions also are given in Fig. 5. A wide variety of interesting and useful forms can be generated and analyzed by the function defined in the foregoing analysis, including bluff bodies, strut forms, and airfoil-type contours at varying angles of attack. The technique does not lend itself to generation of concave or inflected surfaces.

References

[1] Milne-Thomson, L. M., *Theoretical Hydrodynamics* (Macmillan Co., New York, 1950), Chap. XII.

[2] Birkhoff, G. and Zarantonello, E. H., *Jets, Wakes, and Cavities* (Academic Press Inc., New York, 1957), Chap. VI.

[3] Greenhill, G., "Theory of a streamline past a plane barrier," Aeronaut. Research Committee RM19 (1910); also Appendix (1916).

[4] Tulin, M. P. and Burkart, M. P., "Linearized theory for flows about lifting foils at zero cavitation number," David Taylor Model Basin Rept. C-638 (February 1955).

[5] Wu, T. Y., "A free streamline theory for two-dimensional fully cavitated hydrofoils," J. Math. Phys. **XXXV**, 236–265 (October 1956).